Article

Influence of Gold on Hydrotalcite-like Compound Catalysts for Toluene and CO Total Oxidation

Eric Genty, Renaud Cousin *, Sylvie Capelle and Stéphane Siffert

Unity of Environmental Chemistry and Interactions with the Living organisms, University of Littoral Opal Coast, 145 avenue Maurice Schumann, 59140 Dunkerque, France;
E-Mails: Eric.Genty@univ-littoral.fr (E.G.); Sylvie.Capelle@univ-littoral.fr (S.C.);
Stephane.Siffert@univ-littoral.fr (S.S.)

* Author to whom correspondence should be addressed; E-Mail: Renaud.Cousin@univ-littoral.fr;
Tel.: +33-3-2865-8276; Fax: +33-3-2865-8239.

Abstract: X_6Al_2HT500 hydrotalcites, where X represents Mg, Fe, Cu or Zn were synthetized and investigated before and after gold deposition for toluene and CO total oxidation reactions. The samples have been characterized by specific areas, XRD measurements and Temperature Programmed Reduction. Concerning the toluene total oxidation, the best activity was obtained with Au/Cu_6Al_2HT500 catalyst with T_{50} at 260 °C. However, catalytic behavior of Au/X_6Al_2HT500 sample in both reactions depends mainly on the nature of the support.

Keywords: gold based catalyst; hydrotalcite; toluene oxidation; CO oxidation; heterogeneous catalysis

1. Introduction

Volatiles Organic Compounds (VOCs) often cause breathing problems, many of them are carcinogen and they participate in the formation of tropospheric ozone. These VOCs are mainly issued from exhaust of industrial and transport activities. Due to the harm caused to the human environment, the VOCs' emissions are strictly regulated. Among many technologies available for VOCs control, the catalytic oxidation of these pollutants to carbon dioxide and water has been recognized as one of the most promising technologies [1,2]. Complete catalytic oxidation with noble metal supported on solids

is an effective way of VOCs removal at low temperature [3–5]. Moreover, during the past decade, many studies have established that nanosized Au-on-reducible support has a remarkable catalytic activity for many oxidation reactions [3–9]. In a previous work, we have shown that the gold catalyst supported on Ce-Ti mixed oxide prepared by deposition–precipitation method provides a small gold particle size and high catalytic activity in propene oxidation [10,11]. However, in the literature [12], few works have discussed the gold deposition on hydrotalcite for VOCs total oxidation. Thus, an interesting way to obtain mixed oxide catalysts is the use of hydrotalcite precursors. Hydrotalcite-like compounds (HT), a class of layered double hydroxides, consist of positively charged metal hydroxide layers separated from each other by anions and water molecules. The general formula of HT compounds is $[M^{II}_{1-x}M^{III}_{x}(OH)_2]^{x+}$ $[A^{n-}_{x/n}, yH_2O]^{x-}$ where M^{II} and M^{III} are divalent and trivalent metal ions and A^{n-} is an interlayer n-valent anion. Typically, the x value in hydrotalcites is in the range from 0.20 to 0.33 [13,14]. The layers contain metal cations of at least two different oxidation states [13,14]. Indeed, after calcination treatment, mixed oxides are formed and possess unique properties like high specific surface area and porosity, good thermal stability, good mixed oxides homogeneity basic properties and high metal dispersion [15–19]. The partial or total substitution of Mg^{2+} and Al^{3+} is possible by a divalent or trivalent cation in HT structure. It seems interesting to replace the bivalent Mg^{2+} by another efficient element in order to achieve improved toluene and carbon monoxide oxidation.

The copper oxide catalysts are known to be active for the combustion reaction [20–23]. In fact, CuO/Al_2O_3 has shown excellent performance for the total oxidation of CO [20], propene and toluene [21,22]. The iron oxide catalysts are known to be an active solid and support for the CO oxidation [23]. These oxides are recognized to be a good gold support for the VOC oxidation, in particular for the methanol, propanol and toluene oxidation [24]. The gold supported on the zinc oxide was already reported as a good catalyst for the benzene, toluene and xylene oxidation [25]. This solid was reported as having high activity for these reactions compared to the Au/MgO and Au/Al_2O_3.

The aim of the present study is to investigate the effect of gold deposition on X_6Al_2HT hydrotalcites (where X represents Mg, Fe, Cu or Zn) for toluene and carbon monoxide total oxidation reactions. The gold-based catalysts and the supports were characterized by powder X-Ray Diffraction (XRD), BET measurements, UV–visible diffuse reflectance (DR-UV-vis) spectroscopy and hydrogen temperature programmed reduction (H_2-TPR). The gold-based compounds and the mixed oxide derived from HT are tested in catalytic total oxidation of toluene and CO.

2. Results and Discussion

### 2.1. Characterizations of Gold Catalysts and Supports

Table 1 presents the BET specific surface areas of the samples before and after gold deposition. The gold content of the catalysts is mentioned too. After gold deposition, a low decrease of the specific area is observed for all solids. The gold losses in case of Fe_6Al_2HT500 were explained because the pH of the solution was higher than IEP of iron oxide in order to deposit gold in the form of $Au(OH)_3$. In this case, the support is likely to be negative, which leads it to adsorb only the gold cation form and leads to an increase in the losses of gold [3,8].

Table 1. BET surface area and gold content of the solids.

Catalyst	S_{BET} (m².g⁻¹)	Experimental Au content (%)
Mg$_6$Al$_2$HT500	216	-
Fe$_6$Al$_2$HT500	89	-
Cu$_6$Al$_2$HT500	209	-
Zn$_6$Al$_2$HT500	107	-
Au/Mg$_6$Al$_2$HT500	201	3.07
Au/Fe$_6$Al$_2$HT500	87	0.37
Au/Cu$_6$Al$_2$HT500	190	3.15
Au/Zn$_6$Al$_2$HT500	99	2.19

In order to investigate the structure of the samples, XRD patterns were performed (Figure 1). First of all, it could be seen that for the four mixed oxides prepared by the hydrotalcite route, several oxide structures were revealed. Thus, for the compound with magnesium (Mg$_6$Al$_2$HT500) or copper (Cu$_6$Al$_2$HT500), a phase of metal oxide is observed: MgO periclase (JCPDS-ICDD 45-0946) and CuO Tenorite phase (JCPDS-ICDD 48-1548), respectively. Concerning the compound containing iron (and Fe$_6$Al$_2$HT500), the hematite phase (Fe$_2$O$_3$ (JCPDS-ICDD 48-1548)) and magnetite (Fe$_3$O$_4$ (JCPDS-ICDD 48-1548)) are observed in the solid, while for the zinc solids (Zn$_6$Al$_2$HT500), two phases are observed: Zincite phase (ZnO (JCPDS-ICDD 36-1451)) and Gahnite phase (ZnAl$_2$O$_4$ (JCPDS-ICDD 05-0669)).

Figure 1. X-ray diffraction (XRD) patterns of supports and gold catalysts (Δ: MgO; χ: Fe$_2$O$_3$; °: Fe$_3$O$_4$; +: CuO; #: ZnO and ZnAl$_2$O$_4$; * = gold metallic).
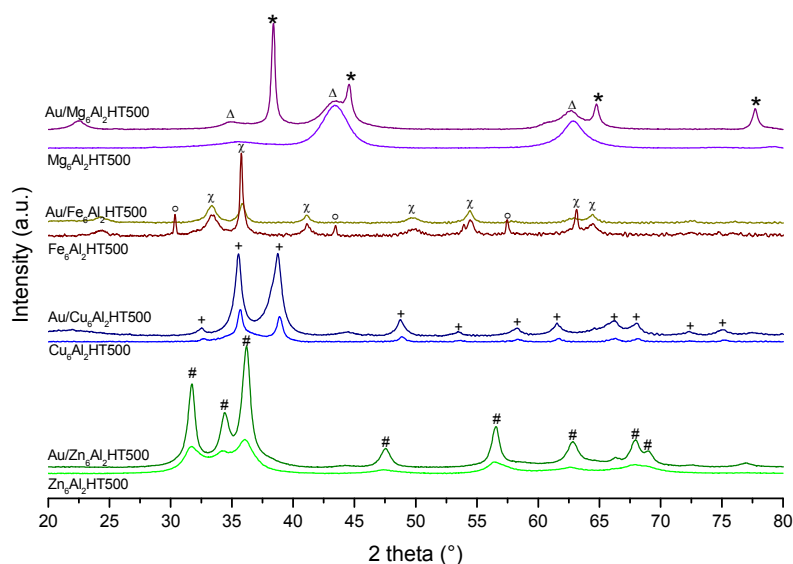

After gold loading, it could be observed that gold deposition affected the oxide crystallinity only for the Au/Fe$_6$Al$_2$HT500. Indeed, for this compound, the Fe$_3$O$_4$ phase was not observed and a decrease of intensity of the others patterns was revealed. An interaction between gold and iron species seems to have occurred. However, concerning the others mixed oxide, same oxide structure of the support has been observed with an increase of the X-ray patterns intensity. For the gold based solids, it is notable that the X-ray diffraction patterns of metallic gold (JCPDS-ICDD 04-0784) at 2θ = 38.2°, 44.4°, 64.5°

and 77.5° are very intense in the case of Au/Mg$_6$Al$_2$HT500 while catalysts with copper (Au/Cu$_6$Al$_2$HT500) and zinc (Au/Zn$_6$Al$_2$HT500) have broad and weak peaks. As regards the compound with iron, no diffraction peak for gold metallic is visible which could be due to this low content in the sample. The difference in the intensity gold diffraction peak between Au/Cu$_6$Al$_2$HT500, Au/Zn$_6$Al$_2$HT500 and Au/Mg$_6$Al$_2$HT500 could be explained by the size of the gold crystallites. An estimation of gold crystallite size was only performed in the case of Au/Mg$_6$Al$_2$HT500 using the Scherrer Equation with the diffraction peak at 2θ = 38.2°. This gold crystallite size was estimated at 15.3 nm. Indeed, for Au/Cu$_6$Al$_2$HT500 and Au/Zn$_6$Al$_2$HT500 the low intensity of X ray diffraction patterns and the overlapping with other signal from several phases did not allow an evaluation of the gold crystallite size. The low intensity of metallic gold X-ray patterns could indicate a high dispersion of gold nanoparticle. This information revealed that the gold dispersion is better in these catalysts.

In order to identify the nature of the gold species, the solids were analyzed by UV-Vis spectrophotometry in diffuse reflectance. The different spectra were presented in Figure 2. The UV-Vis spectra show new bands concerning the gold nanoparticles. Concerning the sample Au/Fe$_6$Al$_2$HT500 beside the support contribution, no clear change in the spectra was observed. However, for Au/Mg$_6$Al$_2$HT500 and Au/Zn$_6$Al$_2$HT500 three absorption bands are detected at 260, 330 and 560 nm. These bands could correspond respectively to: (i) Au$^+$ cations, (ii) (Au)$_n^{\delta+}$ small clusters and (iii) plasmon resonance of Au nanometallic particles [10,26,27]. Indeed, in gold metallic nanoparticles, the plasmon absorption arises from the collective oscillations of the free conduction band electrons that are induced by the incident electromagnetic radiation. This last band was observed on Au/Zn$_6$Al$_2$HT500 at 530 nm. Concerning the band at 330 nm, as in the case of Au/Mg$_6$Al$_2$HT500, this one could be attributed to (Au)$_n^{\delta+}$ small clusters present on the solid. In the case of Au/Cu$_6$Al$_2$HT500, the broad band at around 620 nm could correspond to atoms of edge which are in strong interaction with the support [27].

Figure 2. UV–visible diffuse reflectance (DR-UV-vis) spectra of X$_6$Al$_2$HT500 support and Au/X$_6$Al$_2$HT500 gold based catalysts.
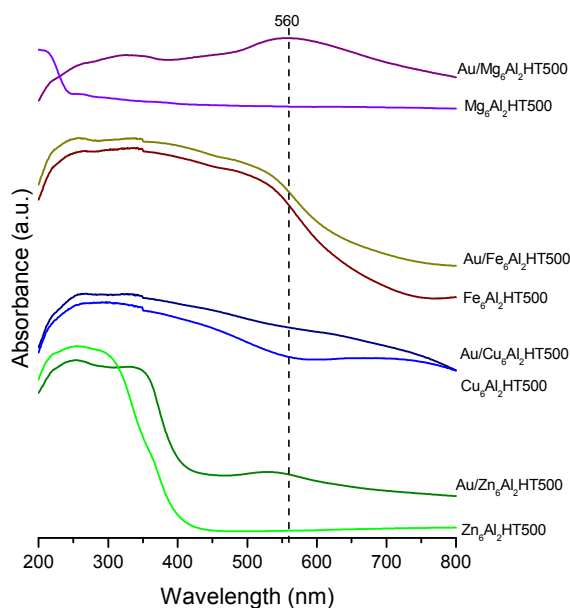
2.2. Catalytic Activity for Toluene and CO Oxidation

A reactivity characterization of the solids has been done for two total catalytic oxidation reactions (toluene and CO). Figure 3 represents the conversion of toluene as a function of the temperature in the presence of catalytic support hydrotalcite (X_6Al_2HT500 where X represents Mg^{2+}, Fe^{2+}, Cu^{2+} or Zn^{2+}) and in the presence of gold-based catalysts (Au/X_6Al_2HT500). When the conversion is complete, H_2O and CO_2 are the only products observed. However, at the beginning of toluene conversion for all samples, a few ppm of benzene are detected. The T_{50} temperatures (temperature for 50% toluene conversion) are reported into the Table 2. According these parameters, a catalytic activity order is established:

$Au/Cu_6Al_2HT500 > Cu_6Al_2HT500 > Au/Fe_6Al_2HT500 > Fe_6Al_2HT500 > Au/Zn_6Al_2HT500 >>$
$Zn_6Al_2HT500 > Au/Mg_6Al_2HT500 > Mg_6Al_2HT500$

Deposition of gold has a beneficial effect on the catalytic activity. Moreover, it could be noticed that the reactivity depends mainly on the nature of the mixed oxides support. The best reactivity is obtained for Au/Cu_6Al_2HT500 ($T_{50} = 260$ °C).

Figure 3. Toluene conversion on mixed oxide supports and gold catalysts *vs.* reaction temperature.
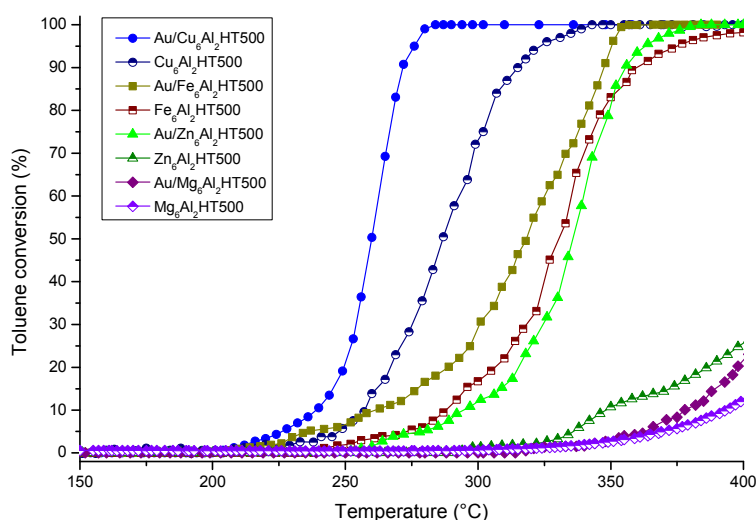
The solids were tested also for the CO total oxidation. The CO total oxidation on gold catalyst could be contributed to a better knowledge of the gold dispersion on the support. The relationship between catalyst activity and gold metallic particle size has been shown by several authors [28–30]. Figure 4 showed the conversion of carbon monoxide as a function of the temperature in presence of mixed oxide and gold based catalysts. According to the T_{50} temperatures (temperature for 50% conversion of carbon monoxide), this catalytic order is established:

$Au/Fe_6Al_2HT500 > Au/Cu_6Al_2HT500 > Au/Zn_6Al_2HT500 > Cu_6Al_2HT500 > Fe_6Al_2HT500 >>$
$Zn_6Al_2HT500 > Au/Mg_6Al_2HT500 > Mg_6Al_2HT500.$

Figure 4. Carbon monoxide conversion on mixed oxide supports and gold catalysts *vs.* reaction temperature.
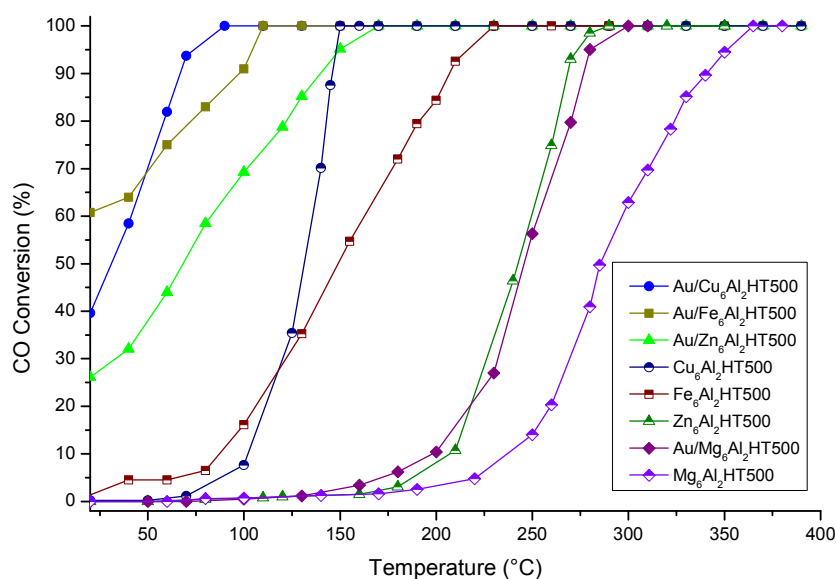
These results show that the gold catalysts are active for the CO total oxidation. The use of gold has a beneficial effect on the activity and depends on the composition of supports. However, good interaction between gold and a support containing copper (Au/Cu$_6$Al$_2$HT500), iron (Au/Fe$_6$Al$_2$HT500) and zinc (Au/Zn$_6$Al$_2$HT500) was also evidenced. It could be noted that the sample showing the lower dispersion (Au/Mg$_6$Al$_2$HT500) by XRD patterns, is less active in the CO total oxidation reaction. Moreover, the solids which have not presented a gold diffraction peak in XRD, showed a greater conversion at room temperature. This information is in accordance with the relationship between the dispersion of gold nanoparticles and catalytic activity for the CO oxidation [28–30].

For a better understanding of the difference in catalytic reactivity between these solids and the redox properties of the best solids, an H$_2$-TPR experiment study was carried out for the solids containing copper and iron.

The results of H$_2$-TPR experiments are reported on the Figure 5 and on the Table 2. Concerning the solid with iron (Fe$_6$Al$_2$HT500), three reduction steps are detected, the first at 354 °C corresponding to the reduction of Fe$_2$O$_3$ into Fe$_3$O$_4$ while the second step (at 610 °C) concurs to the reduction of Fe$_3$O$_4$ into FeO and the last reduction step (at 780 °C) is attributed to the transformation of FeO into Fe^0 metallic [31]. When gold is added to the support, these three reduction peaks are observed in addition to another at 133 °C, corresponding to the reduction of gold species. Concerning the solid with copper (Cu$_6$Al$_2$HT500), three reduction steps are detected. The first (at 201 °C) corresponds to the reduction of highly dispersed CuO species into Cu$_2$O; the second (at 250 °C) is assigned to the reduction of bulk CuO species into Cu$_2$O; the last peak corresponds to the reduction of Cu$_2$O species into metallic copper [32,33]. The adding of gold on the support allows the shifting of the reductions to lower temperatures. This is possible with the increasing of oxygen species mobility on the surface of solids.

Figure 5. Hydrogen temperature programmed reduction (H$_2$-TPR) profiles of X$_6$Al$_2$HT500 support and gold-based catalysts Au/X$_6$Al$_2$HT500.
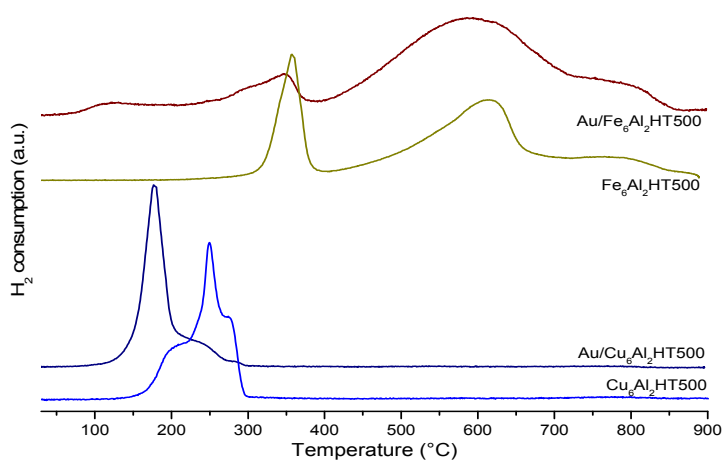

Table 2 resumes the H$_2$-TPR experimental and calculated consumption of gold-based catalysts samples. For calculations of hydrogen consumption during H$_2$-TPR measurement for the gold-based catalysts, if we consider the hypothesis that gold is only in the ionic form Au^{3+}, we could evaluate a maximal H$_2$ consumption from gold species. Thus, knowing the gold content, and taking into account the gold reduction reaction of Au^{3+} into Au°, we could evaluate a theoretical H$_2$ consumption by gold. By subtracting the theoretical consumption of gold from experimental consumption, it could be observed that the H$_2$ consumption of the solids increase when gold is deposited. Indeed, it is known that gold species permit the facilitation of the reduction of oxygen species from the support surface on the border with gold [4,5,10,11]. Thus, in our case, the presence of gold promotes the reduction of iron or copper species at lower temperature and enhances the redox properties of the mixed oxide support prepared by hydrotalcite precursors.

Table 2. H$_2$-TPR consumption and conversion temperature (T$_{50}$) of 50% toluene and CO of catalysts.

Catalyst	T_{50} Toluene oxidation (°C)	T_{50} CO oxidation (°C)	Gold content (%)	Temperature programmed reduction	
				Calculated H$_2$ consumption Au$^{3+}\rightarrow$Au^0 (µmol g^{-1})	Experimental H$_2$ consumption (µmol g^{-1})
Fe$_6$Al$_2$HT500	330	148	-	-	21901
Au/Fe$_6$Al$_2$HT500	324	<20	0.37	28	24437
Cu$_6$Al$_2$HT500	282	130	-	-	10986
Au/Cu$_6$Al$_2$HT500	260	31	3.15	249	13437

The results of the toluene total oxidation could be correlated with the results of the H$_2$-TPR. In fact, the solids with the reduction at low temperature (Au/Cu$_6$Al$_2$HT500 and Cu$_6$Al$_2$HT500) present the best catalytic activity for the toluene oxidation. For the Toluene oxidation, the important point is the

reducibility of the support. Indeed, the importance of the size of the gold nanoparticle is less than in the case of the CO total oxidation. Thus, the gold species enhanced the redox properties of the catalysts which are beneficial for the toluene total oxidation.

Table 3. Results observed for catalytic toluene oxidation with gold-based catalysts.

Catalyst	Toluene concentration (ppm)	GHSV (h^{-1})	T_{50} (°C)	References
Au/Cu_6Al_2HT500	1000	30000	260	This work
$Au/Ce_{0.3}Ti_{0.7}O_2$	1000	30000	260	[10]
Au/TiO_2	1000	16000	372	[34]
Au/TiO_2	1000	35000	321	[35]
Au/Al_2O_3	1000	35000	376	[35]
$Au/CeO_2/Al_2O_3$	1000	35000	279	[35]

A comparison between Au/Cu_6Al_2HT500 (most active sample) and some results reported in other works using gold catalysts and toluene catalytic oxidation were shown in the Table 3 The activity results (T_{50}) obtained by the Au/Cu_6Al_2HT500 close in comparison with best solids from literature [10,34–36]. Despite the difference between operating conditions, the results of the catalysts were very attractive; indeed, the T_{50} obtained for Au/Cu_6Al_2HT500 was better than the other solids.

3. Experimental Section

3.1. Catalysts Preparation and Characterization

Hydrotalcite (HT) like compounds with XAl molar ratio 6:2 (denoted as X_6Al_2HT where X correspond to Mg^{2+}, Fe^{2+}, Cu^{2+} or Zn^{2+}) were prepared by coprecipitation. An aqueous solution containing appropriate amounts of nitrates elements (Mg, Fe, Cu, Zn and Al) was added, under stirring, dropwise into Na_2CO_3 solution. During the synthesis the temperature and pH were maintained respectively at 60 °C and 10 by addition of NaOH solution. The solution was dried at 60 °C during 18 hours. The resulting suspension was filtered off and washed several times with hot deionized water (50 °C) and dried at 60 °C during 48 h. The thermal treatment was performed under flow of air (4 L h^{-1} −1 °C.min^{-1}–4 h at 500 °C). The catalysts are named X_6Al_2HT500 where X corresponds to Mg^{2+}, Fe^{2+}, Cu^{2+} or Zn^{2+}.

Gold-based catalysts were also prepared with the Deposition Precipitation method using sodium hydroxide as precipitating agent. One gram of the hydrotalcite support was added to an aqueous solution at 80 °C containing the suitable amount of gold to obtain 4 weight% in the solid. The pH of $HAuCl_4$ solution was adjusted to 8 by addition of NaOH (0.1 mol L^{-1}) drop by drop under stirring during 4 h. The suspension was filtered, washed several times with hot water in order to eliminate Na^+ and Cl^- ions. The catalyst was then dried in the oven at 80 °C followed by a thermal treatment under air at 400 °C (1 °C min^{-1}) during 4 h. The code names of these catalysts are, respectively: Au/X_6Al_2HT500 (where X represents Mg, Fe, Cu or Zn).

3.2. Catalysts Characterization

To determine the gold content of samples, chemical analysis of Au was performed by inductively coupled plasma atomic emission spectroscopy at the CNRS Centre of Chemical Analysis (Vernaison, France).

The specific surface areas of solids were determined by the BET method using a QSurf M1 apparatus (Thermoelectron), and the gas adsorbed at −196 °C was pure nitrogen.

X-ray diffraction (XRD) measurements were carried out on a Bruker AXS D8 Advance diffractometer equipped with a copper anode ($\lambda = 1.5406$ Å) and a LynxEye detector. The scattering intensities were measured over an angular range of $20° \leq 2\theta \leq 80°$ for all the samples with a step-size of $\Delta(2\theta) = 0.02$ and a count time of 4 s per step. The diffraction patterns have been indexed by comparison with the JCPDS files. Crystallite size of gold nanoparticles was calculated (with a graphics based profile analysis program "TOPAS from Bruker AXS") from the line broadening of the Au diffraction line using the Scherrer equation.

UV–vis diffuse reflectance (UV-vis-DR) spectra were recorded with a Cary 5000 Scan (Varian) spectrophotometer in the spectral range of 200–800 nm.

The temperature programmed reduction (H_2-TPR) experiments were carried out in an Altamira AMI-200 apparatus. The TPR profiles were obtained by passing a 5% H_2/Ar flow (30 mL min^{-1}) through 30 mg of samples heated at 5 °C min^{-1} from ambient temperature to 900 °C. The hydrogen concentration in the effluent was continuously monitored by a thermoconductivity detector (TCD).

3.3. Catalytic Tests

The activity for the toluene total oxidation of the catalysts (100 mg) was measured in a continuous flow system on a fixed bed reactor at atmospheric pressure. Before each test, the catalyst was reactivated in flowing air (2 L h^{-1}) at 400 °C for 4 h. The flow of the reactant gases (100 mL min^{-1} with 1000 ppm of C_7H_8 and balance with air) was adjusted by a Calibrage CALPC-5 apparatus constituted of a saturator and mass flow controllers. After reaching a stable flow, reactants passed through the catalyst bed and the temperature was increased from room temperature to 400 °C (1 °C.min^{-1}). The feed and the reactor outflow gases were analyzed on line by a micro-gas chromatograph (Agilent technologies 490 Micro gas chromatography).

CO oxidation reaction was conducted at atmospheric pressure in a quartz flow microreactor containing 100 mg of catalyst in a fixed bed, using a series of mass flow controllers with diluted gases. The catalytic tests were made using a gas mixture containing 1000 ppm CO and 10% O_2 (He as eluant gas) with a flow of 100 mL min^{-1}, in the temperature range 20–300 °C with a ramp rate 1 °C min^{-1}.

ADEV 4400 IR CO- CO_2 infrared analyzers were used to perform the analysis both CO and CO_2. The catalysts performance was assessed in terms of T_{50} temperature, defined as the temperature, when 50% conversion was obtained.

4. Conclusions

In this study, X_6Al_2HT compounds with several divalent cations are prepared by the coprecipitation method. The samples with gold (Au/X_6Al_2HT500) are synthesized by the deposition-precipitation method. The TPR profiles, XRD patterns and UV-Vis spectra confirm the presence of metallic gold

nanoparticles. The use of gold has a beneficial effect on the catalytic activity for the toluene and CO oxidation. This activity also depends on the composition of the support, particularly the divalent cation. A correlation between catalytic properties and reducibility is observed.

Acknowledgments

Conflicts of Interest

The authors declare no conflict of interest.

References

1. Drago, R.S.; Jurczyk, K.; Singh, D.J.; Young, V. Low-temperature deep oxidation of hydrocarbons by metal oxides supported on carbonaceous materials. *Appl. Catal. B* **1995**, *6*, 155–168.
2. Papaefthimiou, P.; Ioannides, T.; Verykios, X. Combustion of non-halogenated volatile organic compounds over group VIII metal catalysts. *Appl. Catal. B* **1997**, *13*, 175–184.
3. Choudhary, V.R.; Patil, V.P.; Jana, P.; Uphade, B.S. Nano-gold supported on Fe2O3: A highly active catalyst for low temperature oxidative destruction of methane green house gas from exhaust/waste gases. *Appl. Catal. A* **2008**, *350*, 186–190.
4. Scirè, S.; Liotta, L.F. Supported gold catalysts for the total oxidation of volatile organic compounds. *Appl. Catal. B* **2012**, *125*, 222–246.
5. Barakat, T.; Rooke, J.C.; Genty, E.; Cousin, R.; Siffert, S.; Su, B.-L. Gold catalysts in environmental remediation and water-gas shift technologies. *Energy Environ. Sci.* **2013**, *6*, 371–391.
6. Haruta, M.; Kobayashi, T.; Sano, H.; Yamada, N. Novel Gold Caralysts for the Oxidation of Carbon Monoxide at a Temperature far below 0 °C. *Chem. Lett.* **1987**, 405–408.
7. Vargas, J.C.; Ivanova, S.; Thomas, S.; Roger, A.-C.; Pitchon, V. Influence of Gold on Ce-Zr-Co Fluorite-Type Mixed Oxide Catalysts for Ethanol Steam Reforming. *Catalysts* **2012**, *2*, 121–138.
8. Chang, C.-T.; Liaw, B.-J.; Huang, C.-T.; Chen, Y.-Z. Preparation of Au/Mg$_x$AlO hydrotalcite catalysts for CO oxidation. *Appl. Catal. A* **2007**, *332*, 216–224.
9. Dobrosz, I.; Jiratova, K.; Pitchon, V.; Rynkowski, J.M. Effect of the preparation of supported gold particles on the catalytic activity in CO oxidation reaction. *J. Mol. Catal. A* **2005**, *234*, 187–197.
10. Lamallem, M.; El Ayadi, H.; Gennequin, C.; Cousin, R.; Siffert, S.; Aïssi, F.; Aboukaïs, A. Effect of the preparation method on Au/Ce-Ti-O catalysts activity for VOCs oxidation. *Catal. Today* **2008**, *137*, 367–372.
11. Gennequin, C.; Lamallem, M.; Cousin, R.; Siffert, S.; Aïssi, F.; Aboukaïs, A. Catalytic oxidation of VOCs on Au/Ce-Ti-O. *Catal. Today* **2007**, *122*, 301–306.
12. Genty, E.; Cousin, R.; Gennequin, C.; Capelle, S.; Aboukaïs, A.; Siffert, S. Investigation of Au/hydrotalcite catalysts for toluene total oxidation. *Catal. Today* **2011**, *176*, 116–119.

13. Cavani, F.; Trifiro, F.; Vaccari, A. Hydrotalcite-type anionic clays: Preparation, Properties and Applications. *Catal. Today* **1991**, *11*, 173–301.

14. Rives, V. *Layered Double Hydroxides: Present and Future*; Rives, V., Ed.; Nova Science Pub Inc.: New York, NY, USA, 2001; p. 439.

15. Genty, E.; Cousin, R.; Capelle, S.; Gennequin, C.; Siffert, S. Catalytic Oxidation of Toluene and CO over Nanocatalysts Derived from Hydrotalcite-Like Compounds ($X_6^{2+}Al_2^{3+}$): Effect of the Bivalent Cation. *Eur. J. Inorg. Chem.* **2012**, *2012*, 2802–2811.

16. Gennequin, C.; Siffert, S.; Cousin, R.; Aboukaïs, A. Co–Mg–Al Hydrotalcite Precursors for Catalytic Total Oxidation of Volatile Organic Compounds. *Topics Catal.* **2009**, *52*, 482–491.

17. Lamonier, J.-F.; Boutoundou, A.-B.; Gennequin, C.; Pérez-Zurita, M.J.; Siffert, S.; Aboukais, A. Catalytic Removal of Toluene in Air over Co–Mn–Al Nano-oxides Synthesized by Hydrotalcite Route. *Catal. Lett.* **2007**, *118*, 165–172.

18. Jiratova, K.; Cuba, P.; Kovanda, F.; Hilaire, L.; Pitchon, V. Preparation and characterisation of activated Ni (Mn)/Mg/Al hydrotalcites for combustion catalysis. *Catal. Today* **2002**, *76*, 43–53.

19. Kovanda, F.; Jiratova, K.; Rymes, J.; Kolousek, D. Characterization of activated Cu-Mg-Al hydrotalcites and their catalytic activity in toluene combustion. *Appl. Clay Sci.* **2001**, *18*, 71–80.

20. Águila, G.; Gracia, F.; Cortés, J.; Araya, P. Effect of copper species and the presence of reaction products on the activity of methane oxidation on supported CuO catalysts. *Appl. Catal. B* **2008**, *77*, 325–338.

21. Labaki, M.; Siffert, S.; Lamonier, J.-F.; Zhilinskaya, E.A.; Aboukaïs, A. Total oxidation of propene and toluene in the presence of zirconia doped by copper and yttrium. *Appl. Catal. B* **2003**, *43*, 261–271.

22. Tidahy, H.L.; Siffert, S.; Wyrwalski, F.; Lamonier, J.-F.; Aboukaïs, A. Catalytic activity of copper and palladium based catalysts for toluene total oxidation. *Catal. Today* **2007**, *119*, 317–320.

23. Royer, S.; Duprez, D. Catalytic Oxidation of Carbon Monoxide over Transition Metal Oxides. *ChemCatChem* **2011**, *3*, 24–65.

24. Scirè, S.; Minico, S.; Crisafulli, C.; Galvagno, S. Catalytic combustion of volatile organic compounds over group IB metal catalysts on Fe_2O_3. *Catal. Commun.* **2001**, *2*, 229–232.

25. Wu, H.; Wang, L.; Zhang, J.; Shen, Z.; Zhao, J. Catalytic oxidation of benzene, toluene and p-xylene over colloidal gold supported on zinc oxide catalyst. *Catal. Commun.* **2011**, *12*, 859–865.

26. Margitfalvi, J.; Fasi, A.; Hegedus, M.; Lonyi, F.; Gobolos, S.; Bogdanchikova, N. Au/MgO catalysts modified with ascorbic acid for low temperature CO oxidation. *Catal. Today* **2002**, *72*, 157–169.

27. Hosseini, M.; Barakat, T.; Cousin, R.; Aboukaïs, A.; Su, B.-L.; De Weireld, G.; Siffert, S. Catalytic performance of core–shell and alloy Pd–Au nanoparticles for total oxidation of VOC: The effect of metal deposition. *Appl. Catal. B* **2012**, *111–112*, 218–224.

28. Grisel, R.J.; Kooyman, P.J.; Nieuwenhuys, B.E. Influence of the Preparation of Au/Al$_2$O$_3$ on CH_4 Oxidation Activity. *J. Catal.* **2000**, *191*, 430–437.

29. Date, M.; Haruta, M. Moisture Effect on CO Oxidation over Au/TiO$_2$ Catalyst. *J. Catal.* **2001**, *201*, 221–224.

30. Zanella, R.; Giorgio, S.; Shin, C.-H.; Henry, C.R.; Louis, C. Characterization and reactivity in CO oxidation of gold nanoparticles supported on TiO_2 prepared by deposition-precipitation with NaOH and urea. *J. Catal.* **2004**, *222*, 357–367.

31. Yu, Z.; Chen, D.; Rønning, M.; Vrålstad, T.; Ochoa-Fernández, E.; Holmen, A. Large-scale synthesis of carbon nanofibers on Ni–Fe–Al hydrotalcite derived catalysts. *Appl. Catal. A* **2008**, *338*, 136–146.

32. Palacio, L.A.; Velásquez, J.; Echavarría, A.; Faro, A.; Ribeiro, F.R.; Ribeiro, M.F. Total oxidation of toluene over calcined trimetallic hydrotalcites type catalysts. *J. Hazard. Mater.* **2010**, *177*, 407–413.

33. Dow, W.; Wang, Y.; Huang, T. TPR and XRD studies of yttria-doped ceria/-alumina-supported copper oxide catalyst. *Appl. Catal. A* **2000**, *190*, 25–34.

34. Santos, V.P.; Carabineiro, S.A.C.; Tavares, P.B.; Pereira, M.F.R.; Órfão, J.J.M.; Figueiredo, J.L. Oxidation of CO, ethanol and toluene over TiO_2 supported noble metal catalysts. *Appl. Catal. B* **2010**, *99*, 198–205.

35. Ousmane, M.; Liotta, L.F.; Carlo, G.D.; Pantaleo, G.; Venezia, A.M.; Deganello, G.; Retailleau, L.; Boreave, A.; Giroir-Fendler, A. Supported Au catalysts for low-temperature abatement of propene and toluene, as model VOCs: Support effect. *Appl. Catal. B* **2011**, *101*, 629–637.

36. Solsona, B.; Aylón, E.; Murillo, R.; Mastral, A.M.; Monzonís, A.; Agouram, S.; Davies, T.E.; Taylor, S.H.; Garcia, T. Deep oxidation of pollutants using gold deposited on a high surface area cobalt oxide prepared by a nanocasting route. *J. Hazard. Mater.* **2011**, *187*, 544–552.